Fatigue Damage Analysis and Life Prediction of Laminated Metal Plates

R. A. Heller*
Virginia Polytechnic Institute and State University, Blacksburg, Va.
C.T. Liu†
Naval Ordnance Station, White Oak, Md.
and
G.W. Swift‡
Virginia Polytechnic Institute and State University, Blacksburg, Va.

A linear cumulative damage model, using the actual state of stress ahead of a crack in the center layer of a 3-layer, steel-aluminum-steel sandwich material, is used to predict the fatigue life of the plate. The state of stress ahead of the crack tip is calculated from a finite-element method, and is monitored as the crack grows. The model also is applied to a splice joint consisting of aluminum base plates and either aluminum or steel splice joints.

I. Introduction

BONDED sandwich laminates are being used widely in various industries. Both primary and secondary structural components in aircraft and space vehicles will, in the near future, be made of such composites. They also have been successfully used in pipes, chemical tanks, ship hulls, and in other structural applications in which a high strength-to-weight ratio is a desirable feature.

Such materials provide a number of advantages. They can be designed for maximum load carrying efficiency by placing the high strength, high stiffness component in preferential locations. Bonding does not require rivet holes, which are stress raisers and may cause premature failure either under static or fatigue loading. In fact, it has been shown that the fatigue strength of a stiffened panel in an aircraft structure is considerably improved when the stiffeners are bonded to the panel. In the compression design of a stiffened panel, rivets provide discontinuous attachment between the metal sheets and the stabilizing stringers. As a consequence, interrivet buckling may occur causing lower strength for riveted structures. The bonding of damping materials to metal sheets, to form a sandwich structure, currently is being considered as an effective way to control noise-induced fatigue (sonic fatigue) of airframes.

It is well-known that there are imperfections existing in composite materials. These imperfections may be caused by metallurgical defects, or may be produced during the lamination and fabrication process of the structural component. In analyzing the fatigue strength of the material, the localized imperfection may be idealized as a crack in the material. A method of predicting the fatigue life of a cracked, layered composite laminate by using the existing *S-N* curves of the individual materials that comprise the laminate is proposed. The potential application of the proposed crack growth model to the prediction of the fatigue life of various types of structural components is discussed.

The study first will consider the fatigue problem of a bonded laminate composed of three layers of isotropic materials. The two outer layers are made of normalized SAE 4130 steel, whereas the middle layer is 7075-T6 aluminum. It is assumed that the middle layer contains a through crack, located at the center of the layer and perpendicular to the interfaces of the laminate. It also is assumed that the composite laminate is perfectly bonded. Since the crack is through the width of the specimen, and the external loading is uniformly applied at the two ends, it is reasonable to formulate the solution as a plane strain problem. The geometry and detailed dimensions of the specimen are shown in Fig. 1. The model also will be applied to the fatigue failure of splice joints.

II. The Fatigue Damage Model

Fatigue strength is seriously reduced by the presence of a stress raiser such as a notch, hole, or crack. The effect of stress raisers on fatigue generally is studied by comparing the fatigue strength of a smooth specimen to that of a notched specimen at a specific number of cycles. It should be remembered that the theoretical stress concentration factor is based on the local elastic stress, but the actual material behavior near the notch root is complicated by plastic yielding. The

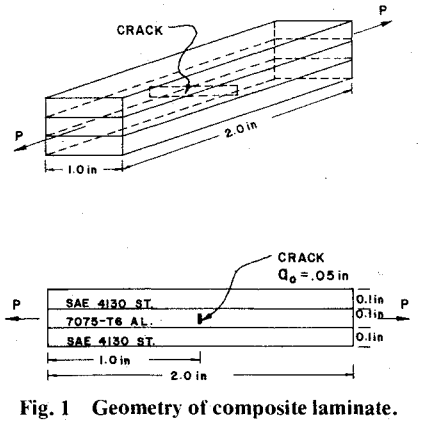

Fig. 1 Geometry of composite laminate.

Presented as Paper 75-768 at the AIAA/ASME/SAE 16th Structures, Structural Dynamics, and Materials Conference, Denver Colo., May 27-29, 1975; submitted June 5, 1975; revision received March 11, 1976. This research has been supported by the U.S. Army, Watervliet Arsenal, under Contract No. DAA-F07-60-C-D444.

Index categories: Aircraft Structural Materials; Structural Composite Materials (including Coatings); Structural Static Analysis.

*Professor of Engineering Science and Mechanics. Associate Fellow AIAA.

†Engineer.

‡Associate Professor, Engineering Science and Mechanics. Member AIAA.

stress state at a crack tip depends on crack geometry, specimen thickness, the material, and the strain hardening rate.

A two-dimensional linear fracture mechanics analysis gives a comprehensive treatment of the elastic stress distribution in the vicinity of a crack. The stress analysis of the crack is much more difficult if plastic yielding substantially disturbs the elastic stress field. The stress and strain state near the crack tip must be determined for nonlinear stress-strain relations, which is possible only for some special geometries and load applications. For example, an analytical elastic-plastic solution of a cracked body, subjected to antiplane loading in longitudinal shear and torsion, has been obtained. However, for the technically important case of tensile loading perpendicular to the crack plane, the exact analytical elastic-plastic solutions are not available at present.

An approximate solution may be obtained, employing some simplified assumptions, such as small scale yielding, a plasticity correction factor, a rigid plastic-strip yielding model, or an analogy with elastic-plastic solutions for longitudial shear.

If the stress distribution at the crack tip is known, a simple crack growth model can be developed. The proposed model is shown schematically in Fig. 2. The material ahead of the crack tip is divided into a number of independent "fatigue elements." Each fatigue element is subjected to the stress distribution in front of the crack tip, and is fatigued according to an octahedral shear stress, $\tau_{oct} - N$ curve for smooth specimens of each individual material. Since the highest stress occurs at the crack tip, it is expected that, after a number of stress cycles with the maximum stress equal to the local stress, the element at the crack tip will fail first. In the proposed crack growth model the crack is presumed to extend by one element width whenever the element fails due to fatigue. Failure of the first element transfers the peak stress to the second element and increases the stresses on the remaining elements. The number of cycles required for failure of the second element and the remaining elements is determined from a linear damage rule. Mathematically, the number of cycles to failure for each element can be expressed as follows:

$$\frac{n_{11}}{N_{11}} = 1 \text{ or } n_{11} = N_{11}$$

= number of cycles to failure of the first element (1)

$$\frac{n_{11}}{N_{12}} + \frac{n_{22}}{N_{22}} = 1 \text{ or } n_{22} = N_{22}\left[1 - \frac{n_{11}}{N_{12}}\right]$$

= number of cycles to failure of the second element (2)

or generally

$$\sum_{i=1}^{j} \frac{n_{ii}}{N_{ij}} = 1 \tag{3}$$

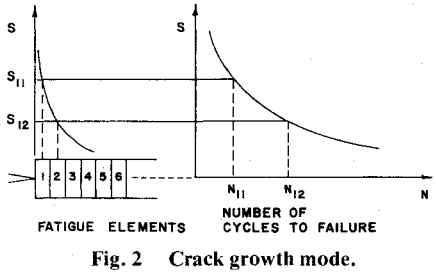

Fig. 2 Crack growth mode.

where n_{ii} is the number of cycles to failure of the ith element when the peak stress is applied to the ith element, and N_{ij} is the allowable number of cycles for the jth element when the peak stress is applied to the ith element. The stress applid to the jth element is obtained from the stress distribution when the peak stress occurs at the ith element. For example, n_{11} = number of cycles to failure of the first element when the peak stress is applied to the first element; N_{12} = the number of allowable cycles for the second element when the peak stress is applied to the first element. The fatigue life of the composite then may be expressed as

$$N_F = n_{11} + n_{22} + n_{33} + \ldots + n_{mm} \tag{4}$$

where m is the total number of elements. In addition,

$$\frac{n_{11}}{N_{12}} \leq 1 \qquad \frac{n_{11}}{N_{13}} + \frac{n_{22}}{N_{23}} \leq 1 \quad \ldots \tag{5}$$

i.e., the quantities on the left-hand side of Eqs. (2) and (3) should be less than or equal to unity. It is assumed that the elements are unaffected by fatigue loading when the stresses are below the endurance limit of the material.

The model incorporated into the linear damage rule will be used continuously until the crack reaches the interfaces. The final failure mechanism of the two outer layers depends on the damage accumulated during the previous stress cycling. If the fatigue element at the interface is fractured either before or at the same time as the crack reaches the interface, a fatigue crack is introduced into the outer layer. This crack serves as a stress raiser, and the same crack growth model will be used to predict the fatigue failure of the outer layer. On the other hand, when the damage accumulation in the first element of the outer layer at the interface is not high enough to cause failure, the crack growth model is not suitable for the description of failure processes in the uncracked layers, because the fatigue damage mechanism in the uncracked layers is similar to that in a smooth specimen. Thus, the failure process in the outer layer involves crack initiation and propagation. A fatigue crack initiation curve is required in order to determine the number of cylces for initiating a crack, and the total life of the outer layer will be the sum of the number of cycles for crack initiation and propagation.

In the presence of a crack, a multiaxial state of stress exists in the material. Since multiaxial stress fatigue data are scarce, an attempt is made to estimate the bi-or triaxial stress S-N curve from uniaxial S-N data. The octahedral shear stress is used to express the state of stress at a point in terms of a single, invariant quantity.

The octahedral shear stress τ_{oct} is related to the yield criterion, which states that yield takes place when the octahedral shear stress is equal to $(\frac{2}{3})^{1/2}$ times the yield stress in pure shear, or $\sqrt{\frac{2}{3}}$ times the yield stress in uniaxial tension. This theory is usually called the distortion-energy theory, and can be expressed, in terms of principal stresses, as

$$\tau_{oct} = \tfrac{1}{3}[(\sigma_1 - \sigma_2)^2 + (\sigma_2 - \sigma_3)^2 + (\sigma_3 - \sigma_1)^2]^{1/2} \geq \tau_{oct\ critical} \tag{6}$$

The possibility of using static failure theories to fatigue failure needs careful investigation, because the nature of fatigue stress is different from that of static stress. Fatigue stress, in general, contains alternating stresses and a static mean stress. The nominal cyclic stresses have been expressed variously as maximum and minimum. In order to assess whether or not the nominal cyclic stress will cause fatigue failure at a given number of cycles, the influence of alternating stresses and superimposed static mean stress should be taken into account.

In order to compare the static failure theories with combined-stress fatigue test data, one may conveniently plot the

amplitude of the alternating principal stresses that cause fatigue failure at a given number of cycles. A simple criterion was proposed by Sines,[1] who stated that the permissible alternation of the octahedral-shear stress is a linear function of the sum of the orthogonal normal static stresses. Mathematically it can be expressed as

$$\tfrac{1}{3}[(\sigma_1-\sigma_2)^2+(\sigma_2-\sigma_3)^2+(\sigma_3(\sigma_1)^2]^{1/2} \leq A-\alpha(S_{m_1}+S_{m_2}+S_{m_3}) \quad (7)$$

where σ_1, σ_2, and σ_3 are the amplitudes of the alternating principal stresses and S_{m1}, S_{m2}, and S_{m3} are the static mean stresses in the principal directions 1, 2, and 3, respectively; A and α are material constants for a given number of stress cycles. Physically, A is proportional to the fatigue strength in completely reversed loading, and α gives the variation of the permissible range of stresses with static stress. This simple theory indicates that in the presence of static tensile stress the permissible alternating stress becomes less, and that in the presence of static compressive stress the permissible alternating stress becomes greater. For biaxial and triaxial stresses, two- and three-dimensional failure surfaces are necessary to represent the failure criterion. In these diagrams, the abscisa is the alternating principal stress P_1, and the ordinate is the other, i.e., P_2. For a biaxial stress state, the failure criterion will plot as an ellipse that has its center at the origin. By variation of the sum of the static stresses, a series of concentric ellipses will be obtained. The size of the ellipse depends on the sum of the static stresses. For large tensile static stresses, the size of the ellipse is reduced. On the other hand, the size of the ellipse will increase with an increase in the negative sume of the static stresses. For a triaxial stress state, the failure surface is a cylinder, the axis of which is the space diagonal with direction cosines $\ell=m=n=\sqrt{1/3}$.

Gough[2] conducted a set of combined bending and torsion tests with and without the superposition of a fixed static bending stress on Ni-Cr-Mo steel. His test results agree with the modified failure criterion, which accounts for the influence of static stress. It should be pointed out that other investigators[3] have found that the algebraic mean stress term $(S_{m1}+S_{m2}+S_{m3})$ does not accommodate typical mean stress effects on fatigue in multiaxially loaded large structures.

Based on the aforementioned discussion of a fatigue failure criterion, the octahedral shear-stress theory provides a reasonable model for predicting fatigue failure. It will, therefore, be used in this study to analyze the fatigue strength of a center cracked composite laminate, and it will be utilized to develop $\tau_{oct}-N$ curves for fatigue under complex loading. The number of cycles to failure for a fatigue element then can be determined once the maximum octahedral shear stress is obtained from a finite-element analysis.

The procedures to develop the $\tau_{oct}-N$ curve are as follows:

1. Determine the octahedral shear stress from Eq. (6). For uniaxial stress σ_y, the octahedral shear stress $\tau_{oct}=0.471\sigma_y$.
2. The $\tau_{oct}-N$ curve is obtained by multiplying the ordinates of the conventional S-N curve of a smooth specimen by 0.471 (Fig. 3).

III. Effects of Residual Stress

Because of the high stress concentration, plastic deformation takes place in the neighborhood of the crack tip. Stresses ahead of the crack tip will be redistributed by plastic deformation. The inelastic deformation upon loading induces a self-equilibrating stress distribution after subsequent external unloading. This stress is know as the residual stress.

Because the octahedral shear stress can be expressed as a function of the second invariant of the stress deviator, which in turn is related to the yield condition, it is practical and convenient to describe the stress state in terms of the octahedral shear stress. The general pattern of the elastic-plastic octahedral shear stress and the residual octahedral shear stress is

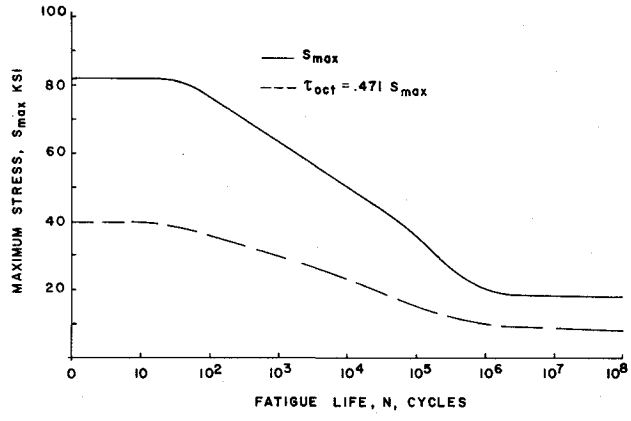

Fig. 3 Conventional S-N curve and derived $\tau_{oct}-N$curve.

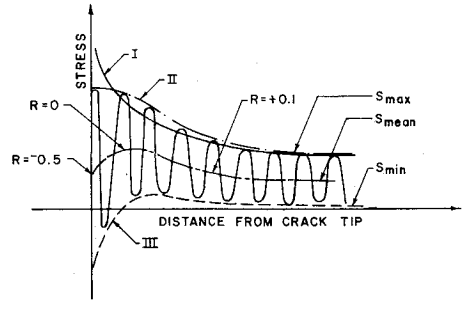

Fig. 4 Residual stress distribution and resulting variable mean stress.

shown in Fig. 4. The elastic distribution shown by curve I is modified by plastic flow to that shown by curve II. Upon removal of the external load, predominantly elastic recovery takes place to produce a residual stress distribution as shown by curve III. When the residual octahedral shear stress is determined, it is assumed that the direction of the octahedral shear stress at a point is unchanged during loading and unloading. Thus, the octahedral shear stresses at a point are superimposed numerically to give the residual octahedral shear stress.

The fatigue behavior of a material will be affected by the presence of residual stresses. The benefical or detrimental effect of the residual stress depends on its magnitude and sign. For fluctuating fatigue loading, if the maximum applied stress is fixed, the resulting compressive residual stress (negative sign) is detrimental, i.e., the fatigue life is reduced. This happens because the material at the crack tip now is subjected to a fluctuating load (with a negative stress ratio) between the compressive residual stress and the maximum plastic stress. As a result, the fatigue crack growth rate is accelerated, and thus the fatigue life of the material at the crack tip is reduced.

The presence of the residual stresses will cause the material ahead of the crack tip to be subjected to a variable amplitude fatigue loading with different stress ratios at every point of the cross-section (see Fig. 4). Those ratios are not the same as the stress ratio of the applied fatigue loading. The stress ratios are determined according to the distributions of the residual stress and the elastic-plastic stresses.

If no plastic deformation occurs, the material ahead of the crack tip is subjected to the same stress ratio as that of the applied cyclic loading. The same situation holds for completely reversed cyclic loading, whether a plastic deformation occurs or not, provided that the tensile yield strength is equal to the compressive yield strength, i.e., the Bauschinger effect is neglected.

On the other hand, if the *amplitude* of the applied cyclic loading is kept constant, then the resulting compressive residual stress will produce a beneficial effect on fatigue, because, for constant stress amplitude, the fatigue life increases with decreasing mean stress. The negative residual

stress will reduce the mean stress of the applied cyclic loading, and thus increase the fatigue life.

When using the proposed crack growth model to predict the fatigue life of a composite laminate, it is important to take the effect of the residual stresses into account. The fatigue elements are subjected to differing cyclic loading with associated stress ratios. The fatigue life of each fatigue element is determined, based on the maximum stress and the stress ratio, by using existing fatigue data. If there is no *S-N* curve with the desired stress ratio available, the Goodman equation

$$\frac{\sigma_a}{\sigma_{ra}} + \frac{\sigma_{\text{mean}}}{\sigma_{\text{ult}}} = 1 \tag{8}$$

will be used to determine an equivalent reversed stress for the element. Here, σ_a = stress amplitude of the fatigue loading, σ_{ra} = stress amplitude of completely reversed fatigue loading, σ_{mean} = mean stress of fatigue load, and σ_{ult} = ultimate tensile stress.

IV. Finite-Element Analysis

One of the most powerful methods of numerical stress analysis, used widely both in research and in practical design, is the finite-element method. By use of this technique, approximate solutions can be obtained for the stress distribution in a wide range of structures with different material properties, complex geometry, and loading conditions.

A general finite-element method for two-dimensional problems, developed by Wilson,[5] has been used in this investigation to calculate the stress field in the cracked composite laminate. The structure under investigation is diveded into a number of discrete elements, which are interconnected at a finite number of nodal points. Each element has 4 nodal points and 8 degrees of freedom. A linear variation of displacement patterns in the x and y directions is assumed. As a consequence, the strains and stresses are constant, and values averaged over the area of the element are obtained at the centroid of each element. The program has the capability to perform elastic-plastic analysis of a complex structure.

The plastic stress is computed from deformation theory whenever an element is in the plastic range. Effective strain is used as the criterion for plastic yielding, i.e., plastic yielding occurs when the effective strain exceeds the yielding strain obtained from a uniaxial tension test. The effective strain is defined as

$$\epsilon_{\text{eff}} = \frac{1}{\sqrt{2}(1+\nu)} [(\epsilon_1-\epsilon_2)^2 + (\epsilon_2-\epsilon_3)^2 + (\epsilon_3-\epsilon_1)^2]^{1/2} \tag{9}$$

where ν is Poisson's ratio and ϵ_1, ϵ_2, and ϵ_3 are the principal strains.

An iterative method is used for elastic-plastic analysis when the deformation theory of plasticity is employed and a bilinear approximation to the stress-strain relation with a non-zero plastic modulus E_p in the plastic region is adopted. The Young's modulus E is modified after each iteration on the basis of a secant modulus. The modified Young's modulus E_{modified} is defined as

$$E_{\text{modified}} = E\left[\left(\frac{\sigma_y}{E\epsilon_{\text{eff}}}\right)\left(1-\frac{E_p}{E}\right)+\frac{E_p}{E}\right] \tag{10}$$

where E = Young's modulus, σ_y = uniaxial yield stress, ϵ_{eff} = effective strain, and E_p = plastic modulus. During the iteration process, each step is treated as an elastic analysis, even though the nonlinear elastic-plastic constitutive relationship is used. The iteration process is repeated until the displacements converge.

Wilson's plane stress finite-element program is modified in order to solve plane strain problems. The program originally was intended for the analysis of noncracked structures and cannot adequately represent the singular stress field at the crack tip. It can, however, be used to obtain approximate solutions with fair accuracy for cracked structures by proper interpretation of the finite-element solution.

The conventional method that is used to analyze a cracked structure is to make the element grid in the vicinity of the

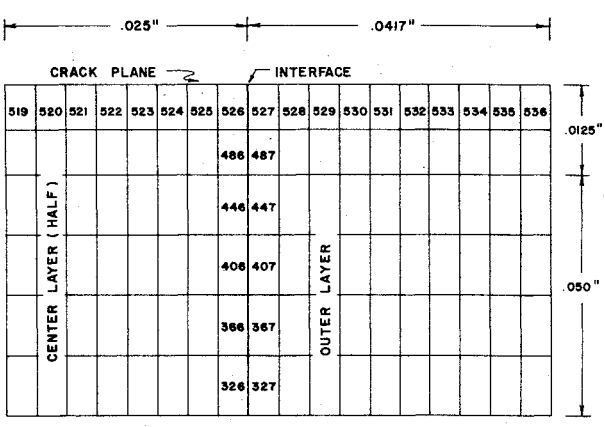

Fig. 5 Finite-element model for one quadrant of laminated plate.

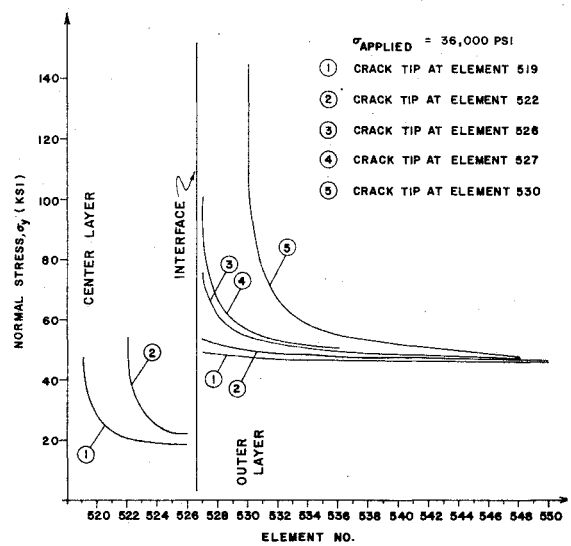

Fig. 6 Normal stress distribution along crack plane as crack propagates (σ_a = 36 ksi).

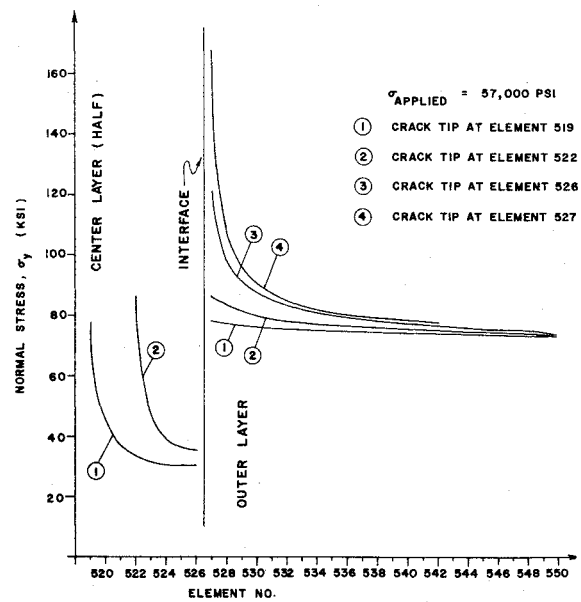

Fig. 7 Normal stress distribution along crack plane as crack propagates (σ_a = 57 ksi).

crack tip extremely fine with a relatively high element concentration near the crack tip. The grid is made fine enough so that the difference between the finite-element solution at a small distance from the crack tip and the classical crack tip stress field obtained from linear elastic fracture mechanics is acceptably small. Using Wilson's program as modified here, the size of the elements along the crack line, called "crack-line elements," is set equal to the size of the element immediately ahead of the crack tip. Because of the symmetry of geometry and applied loading, only one quarter of the composite laminate is analyzed. The shear stress and transverse normal displacement along the vertical center line of the specimen and the shear stress and normal displacement along the horizontal center line of the specimen are zero because of the symmetry conditions. These conditions also provide advantages when the crack propagates; it propagates one element width by releasing the nodal point ahead of the crack tip, i.e., the boundary conditions of the nodal point immediately ahead of the crack tip are replaced by stress free conditions. By so doing, the time-consuming renumbering of nodal points as the crack extends is eliminated. The fourth quardrant of the composite laminate is shown in Fig. 5.

Because the averaged stresses and strains are given at the centroid of each element, and because no element straddles the crack through the thickness of the specimen, the finite-element results apply slightly below the crack plane. The normal stress and the octahedral shear stress ahead of the crack tip and along the crack plane can be obtained by plotting the variation of these stresses in the y direction and extrapolating to the crack plane. Two cases have been examined. In the first, an average far-field stress, $\sigma_a = 36{,}000$ psi has been applied to the composite laminate, whereas in the second, $\sigma_a = 57{,}600$ psi. The normal stress distributions along the crack plane corresponding to the two applied stresses are shown in Figs. 6 and 7. The octahedral shear stress distributions in the crack-line elements, as the crack grows, are presented in Figs. 8 and 9.

V. Delamination

The stress distribution in the composite laminate when a crack is initiated at the interface (delamination) is also obtained from the finite-element program. The normal stress in the crack-line elements as the interfacial crack grows is shown in Fig. 10. The averaged normal and the shear stresses, σ_y and τ_{xy}, located at the centroid of the interfacial elements as an interfacial crack propagates, are presented in Figs. 11 and 12.

According to Fig. 11, the peak stress σ_y in the interface elements decreases as the interfacial crack grows. On the other hand, the shear stress in the interface elements increases with increasing crack length, as shown in Fig. 12. As a consequence, delamination initiated by the normal stress will be propagated by interlaminar shear stresses.

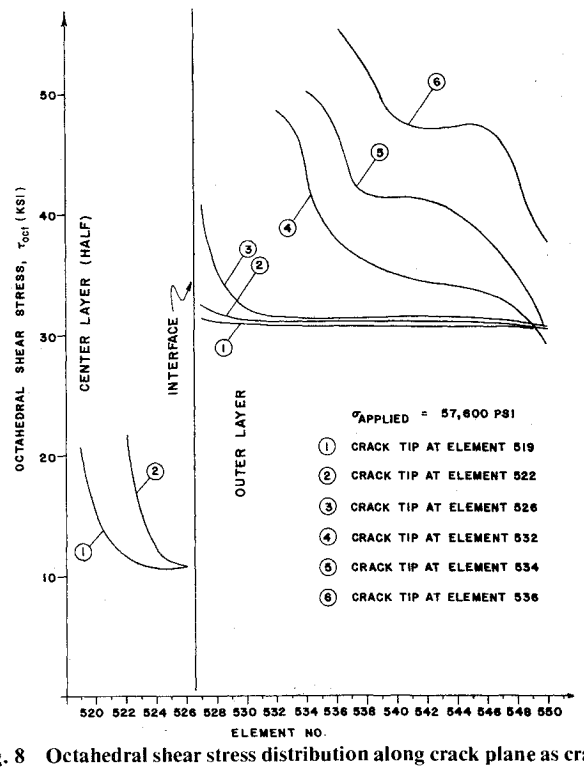

Fig. 8 Octahedral shear stress distribution along crack plane as crack propagates ($\sigma_a = 36$ ksi).

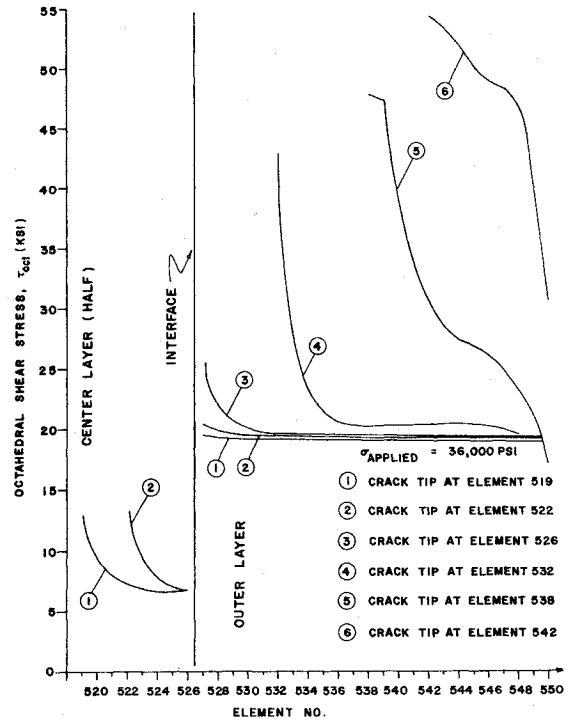

Fig. 9 Octahedral shear stress distribution along crack plane as crack propagates ($\sigma_a = 57$ ksi).

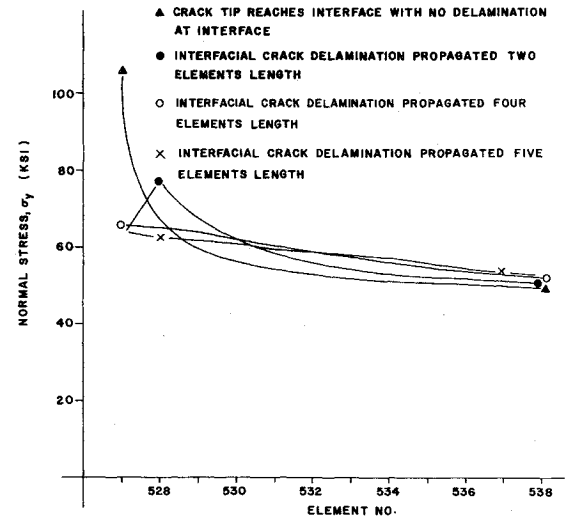

Fig. 10 Normal stress distribution along crack plane as delamination propagates.

VI. Crack Propagation and Fatigue Life Prediction

When a completely reversed, remote, cyclic stress ($R = -1$) of $\sigma_a = \pm 36$ ksi or $\sigma_a = \pm 57$ ksi is applied to the specimen, the actual cyclic stress in each element may be obtained from Figs. 6 and 9. The stress distribution is a function of the advancing crack tip loaction. The number of allowable cycles,

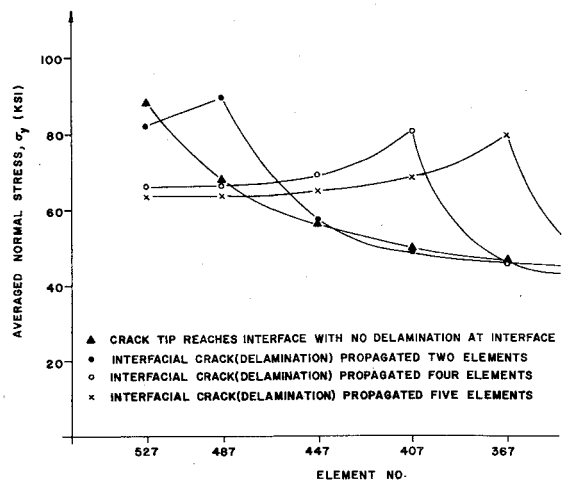

Fig. 11 Normal stress distribution along interface as delamination propagates.

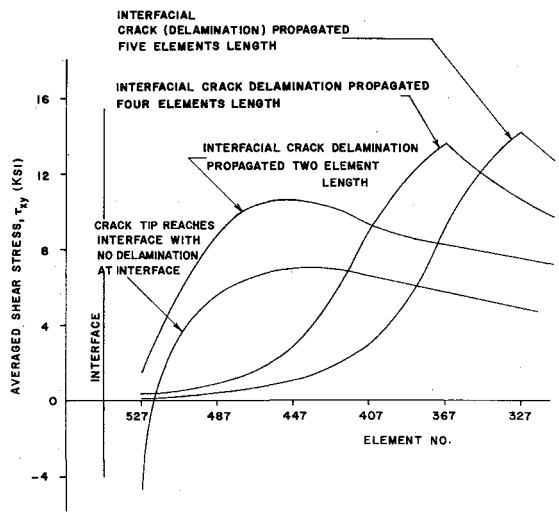

Fig. 12 Shear stress distribution along interface as delamination propagates.

N_{ij}, for each σ_{ij} or τ_{octij} value may then be obtained from the appropriate S-N curve, such as shown in Fig. 3.

These quantities are then introduced into Eqs. (1-5) to obtain the fatigue life of the composite. Because the stress-strain relation used is bilinear, work hardening takes place, and hence, final failure occurs when the length of the crack reaches a critical value, that is when the stress amplitude at the crack tip becomes equal to the ultimate tensile strength, or the octahedral shear failure stress. The material properties for 7075-T6 aluminum and SAE 4130 steel are presented in Table 1.

The predicted fatigue life under a ± 36 ksi reversed stress becomes $N_F = 4.49 \times 10^4$, based on normal stress and $N_F = 205.17 \times 10^4$, based on octahedral shear stress. The stress distribution in the plate is clearly not uniaxial; hence, N_F based on normal stress alone is an unreasonable value.

When calculating the fatigue life, based on the octahedral shear stress, it is not necessary to propagate the crack to its critical length. When the crack length is 7 elements long, shorter than the critical crack length, the life of the fatigue element at the crack tip is 2 orders of magnitude less than the accumulated fatigue life, and therefore is negligible.

For an alternating remote stress of ± 57 ksi, an interesting phenomenon has been observed. Because of the high modulus of the outer layer and the high applied stress, the normal stress and the octahedral shear stress are relatively high in the outer layer. Based on the normal stress, after the crack propagates through two elements in the center layer, the rest of the elements in all layers fail simultaneously, because the normal stress at the crack becomes equal to the ultimate tensile strength. On the other hand, based on the octahedral shear stress, the elements next to the interfaces in the outer layers fail after the initial crack in the center layer propagates through one element. Therefore, new cracks are developed in the outer layers, and the growth of these cracks will compete with the crack in the center layer. Since the stress is relatively uniform in the outer layers and the number of cycles to failure of the first element in the center layer is close to the allowable fatigue life of each element in the outer layers, the damage induced in the outer layers is very high. As a consequence, the elements in the outer layers will fail one by one, and the crack in the center layer stops growing. After the crack propatates through three elements in the outer layers, the fatigue life of the fourth element is 2 orders of magnitude less than the accumulated fatigue life, and is neglected. The center layer will fail at the same time, because alone it cannot sustain such a high applied stress. The predicted fatigue life for this case is $N_F = 88$ cycles based on normal stress, and $N_F = 32640$ cycles based on octahedral shear stress. Again, N_F based on normal stress in unreasonably short because the state of stress is actually multiaxial, whereas the use of the octahedral shear results in a more reasonalbe life estimate. Since experimental octahedral shear-stress-N curves are not readily available, the proposed method of estimating the $\tau_{oct} - N$ curve may be revised once such data are generated.

The propagation of the crack under the two applied stress amplitudes is illustrated in Fig. 13, where crack length is plotted as a function of the number of applied load cycles. The rate of crack growth increases and eventually becomes infinite just before fracture. When the same data are replotted on semilogarithmic paper, as shown in Fig. 14, a straight line results for crack propagation within the central layer. This suggests that the rate of crack growth in this layer is proportional to the crack length:

$$da/dN = Ca \tag{11}$$

Such a linear relation has been proposed by Frost and Dougdale.[7]

VII. Life Prediction for a Splice Joint

The preceding technique also can be applied to the determination of the fatigue life of a splice joint shown in Fig. 15. The joint consists of 7075 T-6 aluminum base plates butted against each other and either aluminum or SAE 4130 steel splice plates. Here the crack is assumed to be the space between the two base plates, and hence its length is equivalent to the thickness of the base plate. As before, the stress

Table 1 Material properties[4]

Material	Ultimate tensile strength, ksi	Yield stress (0.2% offset) ksi	Total elongation, 2-in. gage length, %	Young's modulus, E, ksi	Plastic modulus, E_p ksi
7075-T6 Al.	82.5	76.0	11.4	10400	773
Normalized SAE 4130 steel	117.0	98.5	14.3	29000	838

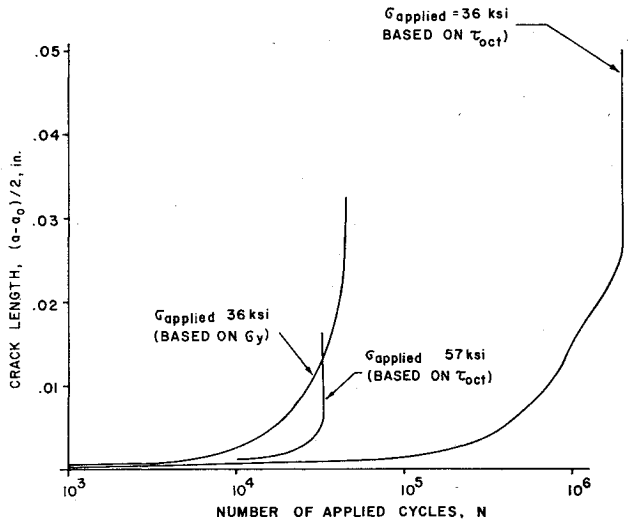

Fig. 13 Crack propagation curves ($a_0 = 0.05$ in).

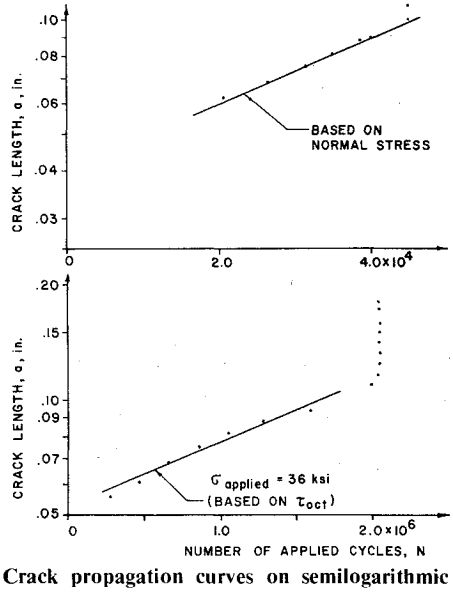

Fig. 14 Crack propagation curves on semilogarithmic scales ($a_0 = 0.05$ in).

distribution of the configuration is analyzed with the aid of the finite-element program, and each element is loaded cyclicly with the appropriate reversed stress amplitude ($R = -1$). Again, using a remote stress of $\sigma_a = \pm 36$ ksi, the life of each joint can be calculated from Eqs. (1-5).

The predicted fatigue life of the A1-A1 splice joint based on normal stress is 165 cycles, and that of the A1-St splice joint is 289 cycles. It should be pointed out however that the fatigue of the A1-A1 splice joint starts at the crack tips in the splice plates, whereas the failure of the A1-St splice joint starts in the base plate at the sharp corners formed by the ends of the splice plates and base plate. This type of failure may be induced in the A1-A1 spice joint also, if it is assumed that the two base plates are not in contact with each other but are separated by a distance equal to the thickness of the base plate. Under such conditions stresses will be largest at the corners of the splice plates and the fatigue life of the joint using normal stress is $N_F = 1316$ cycles.

It may be concluded that the use of steel splice plates has a weakening effect on such joints. This conclusion is confirmed when the octahedral shear stress is used. The fatigue lives of the A1-A1 and A1-St splice joints are, respectively, 25.5×10^3 cycles and 6.54×10^3 cycles. In the design of an actual splice joint, the relative thicknesses of the plates could be varied to reduce such weakening effects.

Again the large difference between results using normal stress and octahedral shear stress are apparent. Although no

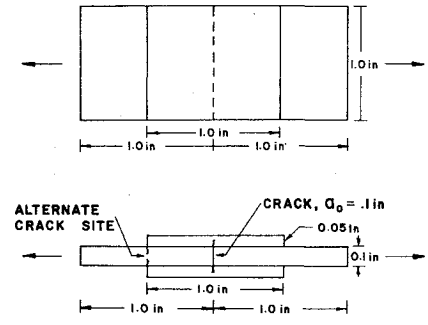

Fig. 15 Geometry of splice joint.

direct experimental data exist for splice joints, the A1-A1 joint may be considered to be a flat, solid, stepped bar with a fillet-type stress concentration at the step.

For the A1-A1 splice joint, the calculated stress concentration factor is $K_t = 1.97$. Therefore, fatigue lives obtained with the proposed analysis may be compared to experimental results for stepped aluminum bars with a $K_t \sim 2$.

The experimental value of $N_{F\,\mathrm{exp}} = 8000$ cycles falls between the life calculated using normal stress, $N_{F\,\mathrm{norm}} = 1316$ cycles, and that obtained with octahedral shear stress $N_{F\,\mathrm{oct}} = 25{,}5000$ cycles. The $N_{F\,\mathrm{norm}}$ value is considered to be unreasonable. Considering the large statistical variations usually observed in fatigue tests, the octahedral shear stress value, although high, is not an unreasonable result.

This estimate is strongly influenced by the assumed $\tau_{\mathrm{oct}} - N$ curve, obtained from a conventional S-N diagram by multiplying the S-N ordinates by 0.471 (see Sec. II). It has been found that reducing the multiplier to 0.45 will result in a fatigue life of about 10,000 cycles, which is much closer to observed lives. Once experimental $\tau_{\mathrm{oct}} - N$ data become available, such calculations may be performed with much greater confidence.

VIII. Conclusions

A cumulative damage mode, which utilizes the elastic-plastic stress distribution ahead of a notch in the central layer of a three-layer composite laminate, has been used to determine crack propagation and fatigue life for the material. Utilizing maximum normal stresses and octahedral shear stresses, two widely differing estimates are obtained. It is believed that the use of normal stress produces an unreasonably low estimate, whereas octahedral shear stress overestimates the number of cycles to failure somewhat. Manipulation of the $\tau_{\mathrm{oct}} - N$ relation results in better correlation with experimental values. The method also has been used to determine crack propagation in splice joints.

References

[1] Sines, G., "Behavior of Metals Under Complex Static and Alternating Stresses," Metal Fatigue, McGraw-Hill, New York, 1959.

[2] Gough, H.J., "Engineering Steels Under Combined Cyclic and Static Stresses," *Journal of Applied Mechanics*, Vol. 17, 1950.

[3] Froerer, D.D. and Goranson, U.G., "Environmental Effects on Fracture Resistant and Biaxial Fatigue Design of Aircraft Structures," *Journal of Engineering Fracture Mechanics*, Vol. 5, No. 3, Sept. 1973, pp. 627-647.

[4] Illg, W., "Fatigue Tests on Notched and Unnoteched Sheet Specimens of 2024-T3 and 7075-T6 Aluminum Alloys and of SAE 4130 Steel with Special Consideration of the Life Range from 2 to 10,000 Cycles," NACA TN 3866, Dec. 1956.

[5] Wilson, E.L., "Finite Element Analysis of Two Dimensional Structures," Ph.D. dissertation, University of California, Berkely (1963); also "Structural Analysis of Axisymmetric Solids," *AIAA Journal*, Vol. 3, Dec. 1965, pp. 2269-2274.

[6] Irwin, G.R., "Analysis of Stresses and Strains Near the End of a Crack Traversing a Plate," *Journal of Applied Mechanics*, Vol. 24, Sept. 1957, pp. 361-364.

[7] Frost, N.E. and Dougdale, D.S., "The Propagation of Fatigue Cracks in Sheet Specimens," *Journal of Mechanics and Physics of Solids*, Vol. 6, 1958, pp. 92-110.